Improved method for calculating projected frequencies along a reaction path

Anwar G. Baboul and H. Bernhard Schlegel

Department of Chemistry, Wayne State University, Detroit, Michigan 48202

Some of the factors affecting the accuracy of following reaction paths and calculating projected frequencies perpendicular to the reaction path have been examined. The S_N2 reaction of Cl^- with CH_3Cl computed at the HF/6-31G* level of theory has been used as a test case. The symmetric C–H stretching mode couples strongly to the reaction path, and the projected frequency of this mode is very sensitive to the numerical accuracy of the path following and frequency projection methods. The transition state geometry must be converged very tightly so that the path steps in the correct direction. For second order implicit algorithms, improved accuracy can be obtained by computing the tangent used for path following and frequency projection from the displacement along the path rather than from the gradient. An even greater increase in accuracy can be achieved by employing the Hessian, used to compute the frequencies, to take a Newton–Raphson step to improve the convergence of the reaction path following. Taken together, these techniques yield a one to three order of magnitude decrease in the errors in the projected frequencies along the reaction path. © *1997 American Institute of Physics.* [S0021-9606(97)00846-5]

INTRODUCTION

Accurate projected frequencies are needed to calculate reaction rates by variational transition state theory[1] (VTST) or reaction path Hamiltonian[2] methods. In these methods, the motion along the reaction path is handled classically, and motions perpendicular to the path are treated quantum mechanically. To obtain the force constants and vibrational frequencies perpendicular to the path, the tangent to the path is used to project out the motion along the path. Thus any inaccuracies in the path or the tangent can lead to errors in the projected frequencies and the reaction rates. In this paper we explore some of the problems of projected frequencies and outline a method for overcoming some of the errors.

Several methods have been developed to follow the minimum energy path (MEP) or intrinsic reaction coordinate (IRC) on a potential energy surface.[3–9] The MEP or IRC is defined as the steepest descent path in mass-weighted coordinates from the saddle point downhill toward reactants and toward products. This definition of the reaction path can be written as a differential equation:

$$\frac{d\mathbf{x}(s)}{ds} = -\frac{\mathbf{g}}{|\mathbf{g}|}, \tag{1}$$

where $\mathbf{x}(s)$ is the reaction path, s is the arc length along the path, and $\mathbf{g}$ is the gradient or first derivative of the potential energy surface. Reaction paths are notoriously difficult to follow accurately.[3–9] Straightforward numerical methods for solving differential equations run into problems since the definition of the reaction path corresponds to a stiff differential equation. Implicit methods are better able to handle stiff differential equations than explicit methods.[10] We have developed a second order implicit algorithm[8] and a family of higher order implicit methods[9] that are capable of following reaction paths with larger step sizes than needed for typical explicit methods.[3–6] In this paper we focus on calculating improved projected frequencies with our second order implicit algorithm, but much of the discussion can be applied to other methods as well. Since steepest descent reaction path following methods must start at the transition state, we also consider how the accuracy of the transition state optimization affects the quality of the reaction path.

The identity S_N2 reaction of chloride with methyl chloride is a suitable test case for exploring the accuracy of projected frequencies,

$$Cl^- + CH_3Cl \rightarrow ClCH_3 + Cl^-. \tag{2}$$

In the transition state, there is significant shortening of the C–H bonds, and hence the symmetric C–H stretching mode participates in the reaction path. As shown below, unless considerable care is taken in the path following and projection, the symmetric C–H stretching frequency can behave rather erratically. Most of the difficulties can be traced to the fact that the gradient is very small in the transition state region, resulting in larger uncertainties in the path following and frequency projection. In this paper we outline methods for overcoming these difficulties and illustrate them with *ab initio* calculations on the chloride plus methyl chloride S_N2 reaction. Similar behavior would be expected if an analytical potential energy surface were used. It should be emphasized that the problems with the projected frequencies are the result of difficulties in reaction path following, and are not due to anomalous features on the potential energy surface. Neither the *ab initio* Born–Oppenheimer surface nor any of the recent analytical surfaces for S_N2 reactions[11,12] show any spurious minima near the transition structure.

METHOD

Second order reaction path following method

In our second order reaction path following method[8] (Scheme 1),
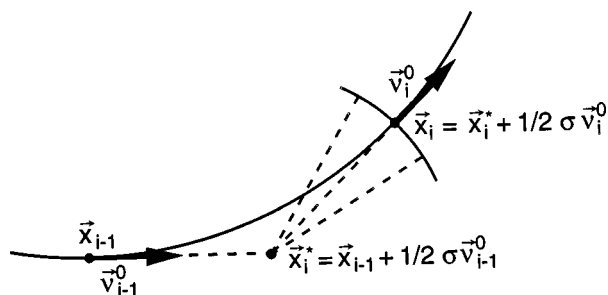
Scheme 1

the path segment between $\mathbf{x}_{i-1}$ and $\mathbf{x}_i$ is represented by an arc of a circle tangent to the gradients at $\mathbf{x}_{i-1}$ and $\mathbf{x}_i$. Since two tangents to a circle form an isosceles triangle, a simple construction allows $\mathbf{x}_i$ to be found by a constrained optimization. A pivot point $\mathbf{x}_i^*$ is obtained by stepping a distance $\sigma/2$ from $\mathbf{x}_{i-1}$ along the tangent at $\mathbf{x}_{i-1}$ (no calculation is performed at $\mathbf{x}_i^*$). Normally the tangent is calculated from the gradient (or from the transition vector if $\mathbf{x}_{i-1}$ is at the transition state and the gradient is zero). A second step of length $\sigma/2$ is taken from $\mathbf{x}_i^*$ to $\mathbf{x}_i$ and the position of $\mathbf{x}_i$ is optimized, subject to the step length constraint, until the gradient is parallel to the step. Equivalently, the energy at $\mathbf{x}_i$ is minimized under the constraint of a fixed step length $|\mathbf{x}_i - \mathbf{x}_i^*| = \sigma/2$. Thus $\mathbf{x}_{i-1}$, $\mathbf{x}_i^*$, and $\mathbf{x}_i$ form an isosceles triangle that by construction is tangent to the path at $\mathbf{x}_{i-1}$ and $\mathbf{x}_i$. Hence, the reaction path between $\mathbf{x}_{i-1}$ and $\mathbf{x}_i$ can be approximated by an arc of a circle. It can be shown that this is a second order algorithm and that it yields the correct curvature at the transition state.[8] This method is similar to the implicit trapezoid method for integrating stiff differential equations;[10] however, we use an optimization to find $\mathbf{x}_i$ more accurately. For the corresponding version of the implicit Euler method (cf. the Muller–Brown method[7]), one would use $\mathbf{x}_i^* = \mathbf{x}_{i-1}$ as the pivot point and $|\mathbf{x}_i - \mathbf{x}_i^*| = \sigma$ as the constraint.

Calculation of the tangent and the projected frequencies

For a point on the path, the tangent to the path can be calculated from the gradient at that point:

$$\nu^0 = \frac{d\mathbf{x}(s)}{ds} = -\frac{\mathbf{g}}{|\mathbf{g}|}, \tag{3}$$

where mass-weighted coordinates have been used throughout. The projected frequencies are then obtained by projecting and diagonalizing $\mathbf{H}$, the mass-weighted Hessian or second derivative matrix,

$$\text{projected } \mathbf{H} = (\mathbf{I} - \nu^0 \nu^{0t})\mathbf{H}(\mathbf{I} - \nu^0 \nu^{0t}). \tag{4}$$

If the gradient is small (e.g., near the transition state), calculating the tangent by Eq. (3) can lead to some uncertainty. A point on the path is obtained by a constrained optimization. The optimization is stopped when the residual gradient perpendicular to the path $\delta\mathbf{g}$, and the change in

TABLE I. Effect of optimization convergence criteria on the HF/6-31G* geometries and energies of $[\text{Cl–CH}_3\text{–CL}]^-$ transition state.

	Regular	Tight	Very Tight
R(C–Cl)	2.383 238 344	2.383 046 72	2.383 044 1
R(C–H)	1.061 073 94	1.061 249 57	1.061 252 68
<HCCl	90.0	90.0	90.0
Total energy	−958.613 461 395	−958.613 461 564	−958.613 461 564

[a]Distances are in angstroms, angles in degrees, and total energies in hartrees.

position, $\delta\mathbf{x}$, are below some reasonable thresholds. When the magnitude of the gradient is small, the residual gradient can cause significant error in the direction of the tangent, i.e., $\nu^0 = -(\mathbf{g} \pm \delta\mathbf{g})/|\mathbf{g} \pm \delta\mathbf{g}|$. An alternative choice is to compute the tangent using the displacement from the pivot,

$$\nu^0 = (\mathbf{x}_i - \mathbf{x}_i^*)/|\mathbf{x}_i - \mathbf{x}_i^*|. \tag{5}$$

This will have less uncertainty, provided $|\mathbf{x}_i - \mathbf{x}_i^*| > |\mathbf{g}|$ and/or $\delta\mathbf{x} < \delta\mathbf{g}$. This form of the tangent can be used to improve the projection in Eq. (4). In addition, Eq. (5) can also be used in the path following to give a better estimate of the next pivot and next point on the path,

$$\mathbf{x}_{i+1}^* = \mathbf{x}_i + \sigma/2(\mathbf{x}_i - \mathbf{x}_i^*)/|\mathbf{x}_i - \mathbf{x}_i^*|$$
$$= \mathbf{x}_i^* + \sigma(\mathbf{x}_i - \mathbf{x}_i^*)/|\mathbf{x}_i - \mathbf{x}_i^*|. \tag{6}$$

Since the Hessian is available at $\mathbf{x}_i$, it can be used to improve the path further. A constrained Newton–Raphson step can be taken to yield a more accurate point on the second order path:

$$\mathbf{x}_i' = \mathbf{x}_i - (\mathbf{H}_i - \lambda\mathbf{I})^{-1}(\mathbf{g}_i - \lambda(\mathbf{x}_i - \mathbf{x}_i^*)), \tag{7}$$

where λ is chosen so that $|\mathbf{x}_i - \mathbf{x}_i^*| = \sigma/2$. The new position $\mathbf{x}_i'$ can be used in Eq. (5) for an improved tangent. The improved tangent and $\mathbf{x}_i'$ can be used to obtain the pivot for the next step along the path via Eq. (6).

Calculations were performed with a modified version of the GAUSSIAN 94 series of programs.[13] Geometry optimization, reaction path following, and projected frequency computations were carried out at the HF/6-31G* level of theory. The chloride–methyl chloride S_N2 reaction has been studied at much higher levels,[14] but the HF/6-31G* level is sufficient to examine the sources of error in reaction path following and frequency projection, and to test the improvements outlined above. Four sets of convergence criteria were used for the geometry optimization and reaction path following. Regular, semitight, tight, and very tight thresholds are to 10^{-4}, 2×10^{-5}, 10^{-5}, and 10^{-6} a.u. for the root-mean-square (rms) gradient (the threshold for the maximum gradient component is 1.5 times larger). The corresponding thresholds for the displacements (in a.u. or rad) are four times the gradient thresholds. A step size of 0.01 amu$^{1/2}$ bohr was used for the present tests.

RESULTS AND DISCUSSION

The transition state geometries optimized with the regular, tight, and very tight criteria are given in Table I. The normal modes for the transition state are illustrated in Fig. 1.
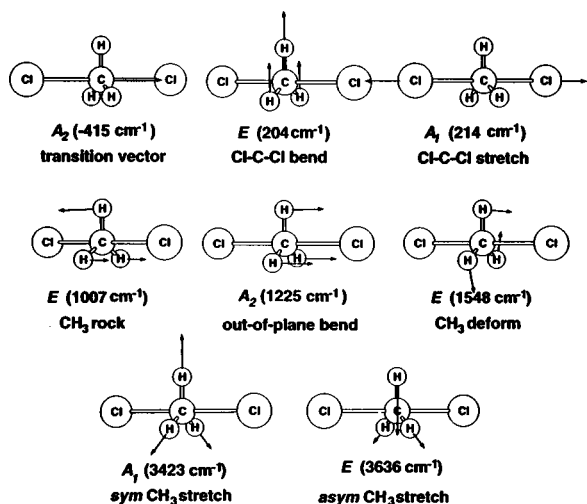
FIG. 1. Normal modes of vibration for the transition state for the S_N2 reaction of Cl^- with CH_3Cl.

The projected frequencies for ~0.2 Å along the reaction path are shown in Fig. 2. The regular convergence criteria have been used for the transition state optimization and the reaction path following, and the tangents for the projection and for stepping along the path have been computed using the gradient, Eq. (3). The symmetric C–H stretching mode shows a 1400 cm^{-1} deep minimum, despite the fact that the potential energy surface is flat and without a minimum in this region. The symmetric Cl–C–Cl also has a minimum (but it is only 15 cm^{-1} deep); all other modes are essentially constant in this region. It is apparent that the projected symmetric C–H stretch is being treated very poorly and the remainder of the discussion concentrates on this mode. The problems can be traced to the convergence of the transition state geometry optimization, the convergence of the path following, and the accuracy of the tangent for the frequency projection. The 1400 cm^{-1} error results from the compounding of these three sources of error. In the following discus-

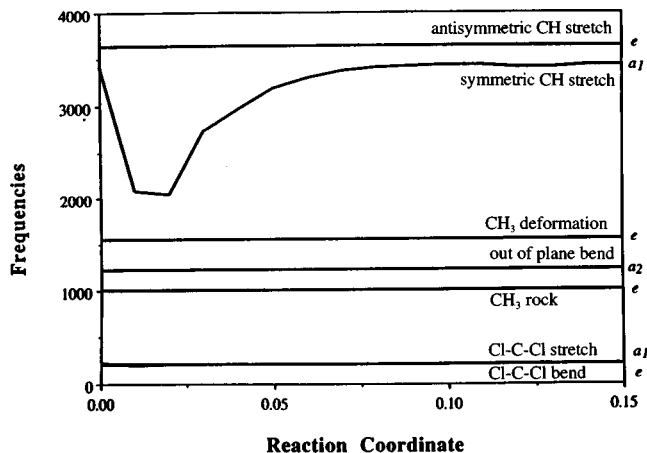FIG. 2. Projected vibrational frequencies for the Cl^-+CH_3Cl S_N2 reaction near the transition state.
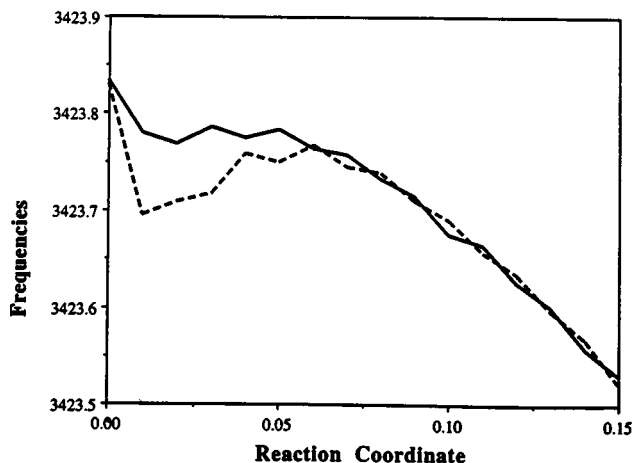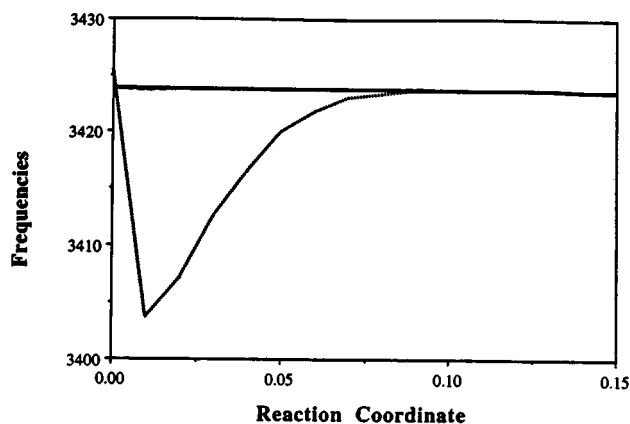

FIG. 3. Effect of transition state optimization convergence on the projected symmetric C–H stretching frequency along the reaction path (regular—dotted, tight—dashed, very tight—solid).

sion, each factor is examined individually, with the errors from the remaining sources greatly reduced (note that the errors are not additive).

Figure 3 shows the effect of optimizing the transition state with the regular, tight, and very tight criteria. In each case very tight optimization was used for the path and the tangent was computed using the gradients. With the regular transition state optimization, there is a 20 cm^{-1} drop in the projected symmetric C–H stretch for the first few points on the path. For the tight and very tight cases, the drop is only 0.1–0.2 cm^{-1}. Unless the transition state has been determined very accurately, a few steps are required to get to the correct reaction path. For these first few steps, the tangent is not parallel to the correct path (particularly in the C–H stretching coordinate in this case), and the projected frequencies are affected. The transition state geometry optimized with very tight convergence is used for the remainder of the discussion.

The convergence of the reaction path optimization also has a major effect on the projected frequencies. Regular convergence results in errors of over 100 cm^{-1} in the projected symmetric C–H stretch. Figure 4 show that the errors for semitight, tight, and very tight convergence are ~4, 0.5, and 0.05 cm^{-1}, respectively, when started from the most accurate transition state geometry. When the optimization criteria are
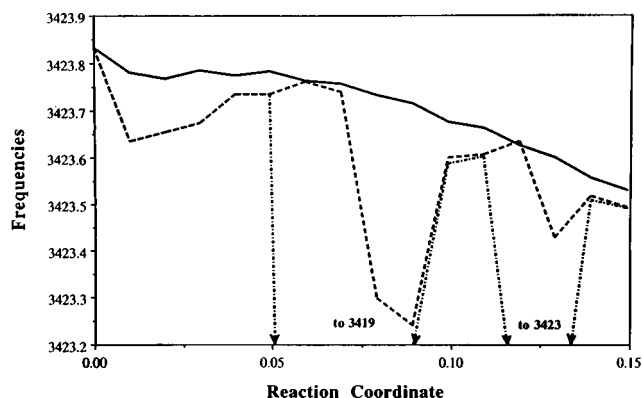
FIG. 4. Effect of reaction path optimization convergence on the projected symmetric C–H stretching frequency along the reaction path (semitight—dot-dashed, tight—dashed, very tight—solid).

not tight enough, the path following algorithm can take a poor step, and several steps may be required to get back to the correct path. Together, a poorly converged step starting from a low accuracy transition state can result in a 1400 cm^{-1} error in the projected C–H stretching frequency. Even the very tight criteria for path following show some undesirable behavior. However, for larger systems and longer reaction paths, it may be too costly to require even tighter convergence.

Some of the remaining problems can be traced to the computation of the tangent. If the displacements are used in Eq. (5) to compute the tangent for the projection, a modest improvement is seen in comparing Fig. 5(a) with Fig. 4. However, much greater improvement is seen when the displacements are also used in Eq. (6) to compute the pivot for the next step along the path. Figure 5(b) shows that the errors in the projected frequencies are a factor of 5–10 smaller than in Fig. 4 or Fig. 5(a). Apparently, inaccuracies in the tangent computed from the gradient cause the path following algorithm to step off the path significantly, resulting in errors in the position of the path, and consequently errors in the projected frequencies.

Further improvement of the accuracy of the reaction path can be achieved by using Eq. (7), a Newton–Raphson step with the analytical Hessian that is needed for the frequencies. Figure 6 shows that the improved paths are smooth and essentially superimposable for the semitight, tight, and very tight convergence criteria. The Newton–Raphson step appears to clean up any remaining errors in the path following for each of the three levels of convergence considered. Even with semitight path optimization convergence, the error in the projected frequency is less than 0.002 cm^{-1}, an order of magnitude better than the original method with very tight convergence criteria, and three orders of magnitude better than with the regular convergence criteria.

CONCLUSIONS

This paper illustrates the importance of accurate calculation of the transition state, reaction path, and tangent for the computation of reliable projected frequencies. For re-
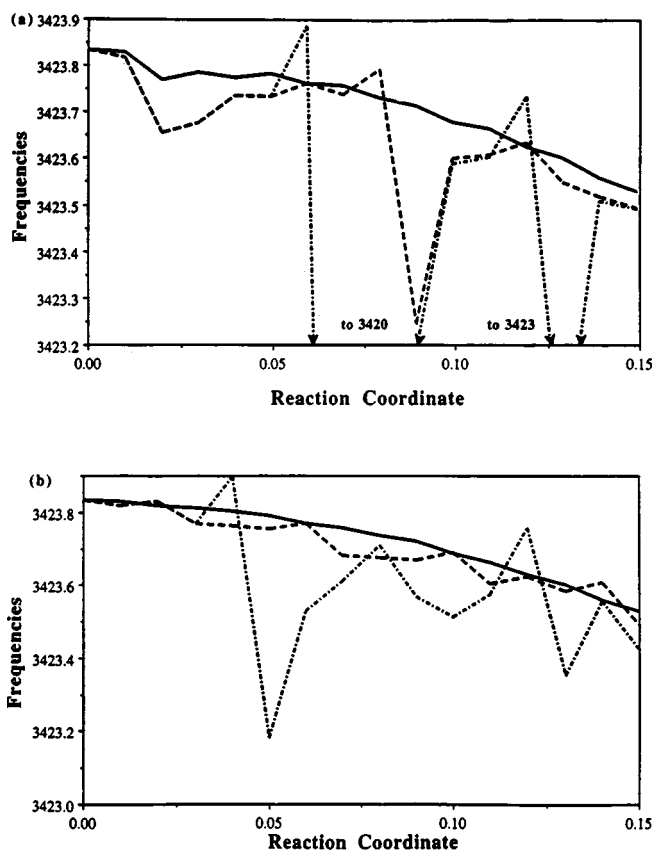

FIG. 5. Effect on the projected symmetric C–H stretching frequency of using the displacements to calculate the tangent for (a) frequency projection only and (b) stepping along the path and frequency projection (semitight—dot-dashed, tight—dashed, very tight—solid).

gions of the potential energy surface where the gradient is small, the tangent for computing the projected frequencies should be calculated from the displacement. In the second order implicit algorithm for reaction path following, the tangent computed from the displacement should also be used for stepping to the next pivot point. Since the Hessian is available from the frequency calculation, it can be used to take a constrained Newton–Raphson step to improve the reaction
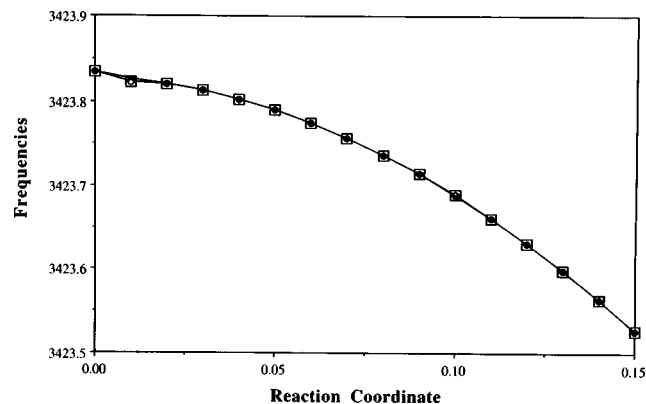

FIG. 6. Effect on the projected symmetric C–H stretching frequency of using the Hessian to take a Newton–Raphson step to improve convergence of the reaction path optimization (semitight—squares, tight—circles, very tight—X).

path and the tangent. This leads to a one to three order of magnitude reduction in the error in the projected frequencies (at essentially no additional cost over the calculation of projected frequencies via the original second order implicit reaction path following algorithm).

The sensitivity of the projected frequencies and the curvature coupling matrix elements to the accuracy of the reaction path and the tangents helps to explain the surprising results of Melissas, Truhlar, and Garrett.[15] They found that the first order (explicit) stabilized Euler method[3] was more cost effective for computing variational transition theory rate constants than a variety of higher order reaction path following methods. For the stabilized Euler method, they use several short steps to calculate the reaction path between Hessian calculations. However, for the second order implicit method, they took only one step and one Newton–Raphson iteration, rather than converging the path accurately. As shown above, careful attention to the accuracy of the path and the tangent is needed for reliable projected frequencies and the needed accuracy can be achieved with very little additional effort.

ACKNOWLEDGMENT

[1] D. G. Truhlar and B. C. Garrett, Acc. Chem. Res. **13**, 440 (1980).

[2] W. H. Miller, N. C. Handy, and J. E. Adams, J. Chem. Phys. **72**, 99 (1980).

[3] K. Ishida, K. Morokuma, and A. Komornicki, J. Chem. Phys. **66**, 2153 (1977); M. W. Schmidt, M. S. Gordon, and M. Dupuis, J. Am. Chem. Soc. **107**, 2585 (1985).

[4] M. Page and J. W. McIver, Jr., J. Chem. Phys. **88**, 922 (1988); M. Page, C. Doubleday, and J. W. McIver, Jr., *ibid.* **93**, 5634 (1990).

[5] B. C. Garrett, M. J. Redman, R. Steckler, D. G. Truhlar, K. K. Baldridge, D. Bartol, M. W. Schmidt, and M. S. Gordon, J. Phys. Chem. **92**, 1476 (1988); K. K. Baldridge, M. S. Gordon, R. Steckler, and D. G. Truhlar, *ibid.* **93**, 5107 (1989).

[6] J.-Q. Sun and K. Ruedenberg, J. Chem. Phys. **99**, 5257, 5269 (1993).

[7] K. Müller and L. D. Brown, Theor. Chim. Acta **53**, 75 (1979).

[8] C. Gonzalez and H. B. Schlegel, J. Chem. Phys. **90**, 2154 (1989); J. Phys. Chem. **94**, 5523 (1990).

[9] C. Gonzalez and H. B. Schlegel, J. Chem. Phys. **95**, 5853 (1991).

[10] C. W. Gear, *Numerical Initial Value Problems in Ordinary Differential Equations* (Prentice-Hall, Englewood Cliffs, 1971).

[11] S. R. Vande Linde and W. L. Hase, J. Phys. Chem. **94**, 2778 (1990); H. Wang, L. Zhu, and W. L. Hase, *ibid.* **98**, 1608 (1994).

[12] S. C. Tucker and D. G. Truhlar, J. Am. Chem. Soc. **112**, 3338 (1990); G. D. Billing, Chem. Phys. **159**, 109 (1992).

[13] M. J. Frisch, G. W. Trucks, H. B. Schlegel, P. M. W. Gill, B. G. Johnson, M. A. Robb, J. R. Cheeseman, T. Keith, G. A. Petersson, J. A. Montgomery, K. Raghavachari, M. A. Al-Laham, V. G. Zakrzewski, J. V. Ortiz, J. B. Foresman, J. Cioslowski, B. B. Stefanov, A. Nanayakkara, M. Challacombe, C. Y. Peng, P. Y. Ayala, W. Chen, M. W. Wong, J. L. Andres, E. S. Replogle, R. Gomperts, R. L. Martin, D. J. Fox, J. S. Binkley, D. J. Defrees, J. Baker, J. P. Stewart, M. Head-Gordon, C. Gonzalez, and J. A. Pople, GAUSSIAN 94, Gaussian, Inc., Pittsburgh, PA, 1995.

[14] M. N. Glukhovtsev, A. Pross, and L. Radom, J. Am. Chem. Soc. **117**, 2024 (1995); S. Seeger, Ph.D. thesis, Cuvillier Verlag, Göttingen, 1995.

[15] V. S. Melissas, D. G. Truhlar, and B. C. Garrett, J. Chem. Phys. **96**, 5758 (1992).